Fuel, Volume 180, 15 September 2016, Pages 514-520
DOI:10.1016/j.fuel.2016.04.050

MODELLING OF SPRAY EVAPORATION AND PENETRATION FOR ALTERNATIVE FUELS

Muhammad Hanafi Azami
Cranfield University
Centre for Propulsion
School of Aerospace, Transport and Manufacturing
Cranfield, Bedfordshire
United Kingdom
MK43 0AL
Email: m.azami@cranfield.ac.uk

Mark Savill
Cranfield University
Centre for Propulsion
School of Aerospace, Transport and Manufacturing
Cranfield, Bedfordshire
United Kingdom
MK43 0AL
Email: mark.savill@cranfield.ac.uk

ABSTRACT

The focus of this work is on the modelling of evaporation and spray penetration for alternative fuels. The extension model approach is presented and validated for alternative fuels, namely, Kerosene (KE), Ethanol (ETH), Methanol (MTH), Microalgae biofuel (MA), Jatropha biofuel (JA), and Camelina biofuel (CA). The results for atomization and spray penetration are shown in a time variant condition. Comparisons have been made to visualize the transient behaviour of these fuels. The vapour pressure tendencies are revealed to have significant effects on the transient shape of the evaporation process. In a given time frame, ethanol fuel exhibits the highest evaporation rate and followed by methanol, other biofuels and kerosene. Ethanol also propagates the farthest distance and followed by methanol and kerosene. However, all biofuels have a shorter penetration length in the given time. These give penalty costs to biofuels emissions formation. The influences of initial conditions such as temperature and droplet velocity are also explored numerically. High initial temperature and velocity could accelerate evaporation rate. However, high initial temperature has resulted in low penetration length while high initial velocity produces contrasting results.

Keywords: evaporation, spray penetration, alternative fuels

NOMENCLATURE

A	Area	m^2
CA	Camelina Biofuel	
c_d	Drag Coefficient	
$c_{i,s}$	Vapor Concentration at Droplet Surface	$mol/s.m^2$
c_p	Constant Pressure Specific Heat	$J/kg.K$
$D_{i,m}$	Diffusion Coefficient of Vapour in the Bulk	m^2/s
D_o	Nozzle Diameter	m
d	Diameter	m
ETH	Ethanol Fuel	
h	Convective Heat Transfer Coefficient	W/m^2K
h_{fg}	Latent Heat	J/kg
JA	Jatropha Biofuel	
KE	Kerosene Fuel	
k_c	Mass Transfer Coefficient	m/s
k_∞	Thermal Conductivity of Continuous Phase	$W/m.K$
MA	Microalgae Biofuel	
MMD	Mass Median Diameter	m
MTH	Methanol Fuel	
MW	Molecular Weight	kg/mol
m	Mass	kg
N_i	Molar Flux of Vapor	mol/m^2s
Nu	Nusselt Correlation	
P	Pressure	Pa
P_{sat}	Saturation Vapor Pressure	Pa
Pr	Prandtl Number of Continuous Phase	
R	Specific Gas Constant	$J/kg.K$
Re	Reynolds Number	
R_u	Synthesized Paraffinic Kerosene	$J/kmol.K$
r	Radius	m
Sc	Schmidt Number	
SMD	Sauter Mean Diameter	m
s	Penetration Distance	m
T	Temperature	K

T_g	Temperature of Continuous Phase	K
t	Time	s
V	Velocity	m/s
α	Volume Fraction of Droplet Spray	
θ	Half Angle of Spray Cone	°
ρ	Density	kg/m^3
μ	Molecular Viscosity	$kg/m.s$
∀	Volume	m^3
SUBSCRIPT		
P	Droplet Particle	

1. INTRODUCTION

Two separate important issues need to be addressed: (1) the environment crisis due to global warming and (2) the energy crisis that leads to the increase of global oil prices. Over time, the spike in global oil price will affect the domestic energy situation as well as impact the local society life [1]. International Energy Agency (IEA) has reported that the world will need 50% more energy in 2030 than it needs today [2], with the transportation sector becoming the second largest energy-consuming sector after the industrial sector. Nearly all fossil fuel energy consumption in the transportation sector is obtained from fossil fuels (more than 90%) with a small amount from natural gas and renewable energy sources [3,4]. However, as the demand for energy increases, the conventional oil and natural gas reserves that can be commercially exploited will diminish after approximately 41.8 and 60.3 years respectively [2].

Much effort has been employed to discover alternatives fuel sources which are sustainable, practical, nature friendly and reliable. These include the usage of biodiesel and biofuel. Biofuel is defined as a fuel comprised of mono-alkyl esters of long-chain fatty acids derived from renewable resources that can be produced by a simple chemical process known as transesterification. Transesterification is a process where the triglycerides react to alcohols in the presence of a catalyst [5] using edible, non-edible, waste vegetable oils and animal fats produced by organism [2,6,7]. Meanwhile, biodiesel (methyl or ethyl

ester) is commonly used among biofuels which is considered as a very promising fuel in transportation. It possesses similar properties as diesel fuel and is miscible at any proportion of the fuel mixture [5] without producing any changes in the existing distribution infrastructure of the fuel [8]. Biodiesel is a non-toxic fuel that is ecological, uncontaminated and emits lesser pollutants. However, the main problem associated with the use of biodiesel is the high production cost (largely owing to the high cost of the feedstock). The use of biodiesel is steep and can be difficult due to its susceptibility to oxidation difficulties and poor low-temperature properties [8].

Despite that, increasing the thermal efficiency can optimize the combustion process and reduce the emission at the same time [9]. One of the methods is by spray characteristics. Spray behaviour is a critical factor in an engine performance [10] such as spray atomization and spray penetration. Spray atomization is a process which involves breaking-up the bulk of liquid jets into small droplets using atomizer or nozzles [9]. Meanwhile, spray penetration is defined as the propagation of droplet until it is fully vaporized. Liquid sprays are formed by discharging liquid at a high velocity from a nozzle. The use of spray is versatile as it can be used for agriculture, internal combustion engine and gas turbine combustors. Liquid that has a high discharge velocity will induce break-up streams to droplets and ensure enough inertial forces to transfer momentum, matter and heat effectively to the gas environment [11]. Spray zones can be classified into three zones; (1) at the nozzle tip where liquid discharge velocity is much larger than the stream velocity, (2) forced jet zone where the droplets' velocity decelerate and is comparable to stream's velocity, and (3) falling droplet zone where the droplets' velocity is lower than the terminal velocity [11,12].

2. LITERATURE REVIEW

This section discussed on the overview of works which have been done that are related to spray behaviours. Chen et al. [10] have classified fuel spray behaviours into two categories: (1) macroscopic conditions and (2) microscopic conditions. They further added that macroscopic parameters include spray tip

penetration and cone angle while the microscopic parameters are related to droplet velocity, droplet size and size distribution. From their macroscopic spray properties point of views, spray tip penetration is directly proportionate to the injection pressure, time duration and higher blend of biodiesel mixing ratio. However, higher blending ratio will result in a smaller cone angle, a small area and volume but higher velocity of spray. These lead to a reduction of quality in spray atomization. In contrary, spray tip penetration is inversely related to the ambient pressure. As the ambient pressure is increased, the spray cone angle will become larger. Furthermore, spray volume is increased as the injection pressure is increased until it reaches a certain limit.

Meanwhile, from microscopic spray properties point of view, the Sauter Mean Diameter (SMD) of the droplet is increased at a higher ambient pressure, radial and axial distance from the nozzle tip and at higher blending mixing ratio. However, a higher blend of mixing ratio will result in a more concentrated fuel distribution, larger droplet Mass Median Diameter (MMD) and span factor due to higher viscosity and surface tension. In contrary, higher injection pressure will reduce SMD but will increase the peak droplet's size volume frequency distribution. The reduction in droplet's diameter and the increase of the temperature of the surface were found to be strongly dependent on the fuel properties. For faster vaporization rate of the droplets, the fuel should have a combination of higher vapour pressure, lower latent heat thermochemical properties [13], low viscosity, low surface tension, low density [9] and low boiling point. They also added that pre-heating process could improve the vaporization performance of the SMD reduction.

Yule & Filipovic [14] have predicted the break-up length which refers to the distance of fully atomized droplet which is equivalent to 35% of the penetration length. Later, Ryu et al. [15] showed that the spray penetration length is directly proportional to the power of ¼ of back pressure. They also added that the spray impingements with ambient density have a greater influence on fuel evaporation and fuel mixture as compared to pressure and temperature intake condition. Concurrently, Chen et al. [10] included that the break-up length is increased with a larger diameter of nozzle but reduced at a higher injection pressure. For the time variant of spray penetration, Kostas et

al. [16] found that spray tip penetration is proportional to the time power of 3/2 during the early stage until it reaches maximum velocity. However, they added that the spray tip velocity is found to be the square root of time at the same stage. Lee & Park [17] have studied both experiment and numerical analysis of fuel break-up using Kelvin-Helmhotz (KH) and Rayleigh-Taylor (RT) hybrid model in high-pressure diesel injection sprays. They discovered that KH breakup occurred near the injector while RT occurred at the secondary breakup and is distributed wider. For further improvement, Roisman et al. [18] have included the shock wave propagation in the air after the injection stage in their paper. Normal adiabatic shock wave has shown the impact to the tip velocity right after the injection stage.

Based on many numerical analysis and experimental works done by researchers to characterized micro and macroscopic droplet atomisation and penetration process, rarely have been studied on different type of alternative fuels. This is equally important to underline the issue of environmental sustainability as well as to understand the behaviour of these alternative fuels. The main objective of this study is to model the transient condition of atomization and spray penetration process using six different alternative fuels, namely, Kerosene, Ethanol, Methanol, Microalgae biofuel, Jatropha biofuel, and Camelina biofuel. The comparisons of thermochemical properties are also presented to perform the atomization analysis of the fuels. A transient condition of atomization and spray penetration process are illustrated. Furthermore, transient variations of temperature and droplet density are included for the analysis. This includes analysing the correlation between the effect of vapour pressure and the evaporation process. The difference between the present study and [19] is on how the modelling is conducted. As an extension of their work, different alternative fuels are used for the analysis. Furthermore, to the best of the author's knowledge, this study is the first to analyze the atomization and spray penetration of Microalgae biofuel. The analytical comparisons are essential as this '3rd generation' of biofuels has been commercialized and are mainly used for aviation purposes.

3. METHOD

In the beginning, initial conditions are defined. These include the temperature, velocity, diameter and volume of the particle. The ambient conditions are also specified such as velocity, temperature, density, pressure and viscosity of the gas. These initial conditions are tabulated in Table 1. For comparison purposes, several thermochemical properties are used as shown in Table 2.

Table 1 Initial Conditions Parameter

Properties	Value
$T_P\,(K)$	294.15
$V_p\,(m/s)$	100
$d_P\,(m)$	2E-5
$\forall_P(m^3)$	4.19E-15
$r_P\,(m)$	1E-5
$V_g(m/s)$	0
$T_g\,(K)$	1000
$\rho_g\,(kg/m^3)$	0.353
$P_g\,(Pa)$	101325
$\mu_g\,(m^2/s)$	4.27E-5

Table 2 Thermochemical Properties

	KE	ETH	MTH	MA	CA	JA
$MW\,(kg/mol)$	0.182	0.046	0.032	0.169	0.156	0.157
$h_{fg}\,(kJ/kg)$	251	846	1100	251*	251*	251*
$c_p\,(J/kg.K)$	2010	2300	2510	2010*	2010*	2010*
$k_g\,(W/m.K)$	0.15	0.17	0.17	0.15*	0.15*	0.15*
$\rho_p\,(kg/m^3)$	810	789	792	755.2	753	749
$\mu_p\,(N.s/m^2)$	0.0016	0.0011	0.0006	0.0039	0.0033	0.0037

*[20]

Modelling an evaporation process is necessary to ensure the fuels are completely vaporized in the mixture before they are burned. Equations in FLUENT Manual book are used to simulate the process. In FLUENT, the droplet trajectory is predicted by integrating drag force, gravitational force and other additional force acting on the droplet. In order to assess the evaporation process of droplets, few assumptions addressed by Mazlan [22] are listed below with few modifications on the modelling:

1. The droplet is a spherical single droplet;

2. The initial droplet diameter was defined;
3. No radiation heat transfer was included during the evaporation process;
4. Gas is stagnant and the droplet is evaluated in a stationary condition;
5. The bulk mole fraction of those fuels is assumed as zero, as we are considering that the fuel is evaporating in pure air.

From the above assumptions, it is noted that droplets produced by a pressure swirl atomizer is initially a well-defined spherical droplet. With the exception of radiation heat transfer, only convection heat transfer is considered. Practically, radiation heat transfer will be considered when the system at high pressure and temperature. Considering that the fuel is evaporating in pure air, molar flux of droplet's vapour in equation (14) is reduced and term $c_{i,\infty}$ is equal to zero.

Reynolds number is defined as:

$$Re_p = \frac{\rho d_p (v_p - v_{\bowtie})}{\mu_p} \tag{1}$$

Meanwhile, the drag coefficient is reduced through [21]'s particle trajectory of two-phase flow system:

$$c_d = \frac{24}{Re_p}\left(1 + \frac{Re_p^{\frac{2}{3}}}{6}\right) \tag{2}$$

Neglecting gravitational and additional forces, motion of the particle is described as:

$$\frac{dv_p}{dt} = \left(\frac{18\mu}{\rho_p d_p^2}\right)\left(\frac{c_d Re_p}{24}\right)(v_\infty - v_p) \tag{3}$$

Since Reynolds number and Prandtl number are known, Nusselt number is calculated by utilising the Ranz-Marshall correlation [13]:

$$Nu = 2.0 + 0.6 Re_p^{\frac{1}{2}} Pr^{\frac{1}{3}} \tag{4}$$

Convective heat transfer relation is then calculated as a function of mass transfer coefficient:

$$h = \frac{Nu.k_{\infty}}{d_p} \tag{5}$$

The area and the mass particle are simply calculated as:

$$A_p = 4\pi r_p^2 \tag{6}$$

$$m_p = \rho_p \forall_p \tag{7}$$

By rearranging the Nusselt number with the function of Reynolds number, Schmidt number is obtained as:

$$Sc = \left(\frac{Nu - 2.0}{0.6 Re_p^{\frac{1}{2}}} \right)^3 \tag{8}$$

By obtaining Schmidt number and Nusselt number, diffusion coefficient of vapour pressure in the bulk and mass transfer coefficient are then calculated:

$$D_{i,m} = \frac{\mu_p}{\rho_p Sc} \tag{9}$$

$$k_c = \frac{Nu.D_{i,m}}{d_p} \tag{10}$$

Numerically, Kerosene saturation vapour pressure is obtained from this correlation [19]:

$$P_{sat} = 1886058.95e\left(\frac{-4576.45}{T_p}\right) \tag{11}$$

For Ethanol and Methanol, Antoine equations are used where A, B and C coefficients are tabulated in Table 3.

Table 3 Antoine Coefficients

	A	B	C
Ethanol	8.04494	1554.3	222.65
Methanol	7.97328	1515.14	232.85

$$\log_{10} P^{sat}(mmHg) = A - \frac{B}{T(℃) + C} \tag{12}$$

The concentration of vapour at the surface of the droplet was calculated by assuming that the partial pressure of vapour at the interface is equal to the saturated vapour pressure at the particle droplet temperature.

$$c_{i,s} = \frac{P_{sat}}{\mathcal{R}T_p} \tag{13}$$

Therefore, the molar flux of droplet's vapour is calculated by using this relation as stated in equation (14). The molar flux of droplet's vapour corresponds to the difference in the concentration of vapour between the droplet surface and bulk gas [19].

$$Ni = k_c(c_{i,s} - c_{i,\infty}) \tag{14}$$

As the condition of fuel's droplet temperature is less than the boiling temperature, the change of mass is then calculated using this relation:

$$\frac{dm_p}{dt} = -NiA_pMW_p \tag{15}$$

The change of temperature in fuel's droplet is calculated from the heat balance and assuming that no radiation heat transfer occurs, the equation from FLUENT can be rearranged as follows:

$$\frac{dT_p}{dt} = \frac{hA_p(T_g - T_p) + \frac{dm_p}{dt}h_{fg}}{m_p c_p} \tag{16}$$

For the next time step, these relations are used:

$$v_{p_2} = v_{p_1} + \frac{dv_{p_1}}{dt}dt \tag{17}$$

$$m_{p_2} = m_{p_1} + \frac{dm_{p_1}}{dt}dt \tag{18}$$

$$T_{p_2} = T_{p_1} + \frac{dT_{p_1}}{dt}dt \tag{19}$$

By using conservation of mass, the new particle area, the radius and the diameter can be calculated using these relations:

$$A_{p_2} = \frac{\dot{m}_2}{\rho_{p_2}v_{p_2}} \tag{20}$$

$$r_{p_2} = \left(\frac{m_{p_2}}{4/3\pi\rho_{p_2}}\right)^{\frac{1}{3}} \tag{21}$$

$$d_{p_2} = 2r_{p_2} \tag{22}$$

Lastly, to simulate at every time step, all the equations above are repeated until the mass and velocity turned to zero which indicates that the droplet has been fully vaporized. Spray penetration determines the propagation distance of a

droplet in the combustor. To predict the length of penetration of the droplet, Mazlan [22] and Sazhin et al. [12] have recommended to use this length penetration relation:

$$s = \frac{\sqrt{V_i D_o t}}{(1-\alpha_d)^{1/4}\tilde{\rho}^{1/4}\sqrt{\tan\theta}}\left(1 - \frac{\sqrt{D_o}}{4\sqrt{V_i(1-\alpha_d)^{1/4}\tilde{\rho}^{1/4}\sqrt{\tan\theta}\sqrt{t}}}\right) \quad (23)$$

Where s is the distance measured from the nozzle, $\tilde{\rho} = \frac{\rho_a}{\rho_d}$ is the dimensionless parameter. Taking D_0 = 1mm, θ = 34.89^0 and $\alpha_d = 1e^{-4}$, the spray length penetration of each fuel can be calculated.

4. RESULTS AND DISCUSSION

4.1 Atomization and penetration of alternative fuels comparison

In this section, the predictions of the developed spray atomization and penetration model results are reported. Firstly, it is worth mentioning that the model validation is comparable to the model developed by Sazhin et al. [12] for spray penetration and Ghassemi et al. [23] for atomization general behaviour.

The variations of vapour pressure as the function of temperature for all fuels are calculated prior to the analysis. This is done because the vapour pressure has a strong dependence on the temperature and the thermochemical properties of the fuel. All fuel show an increase in vapour pressure as the temperature increases until it achieves a certain limit. As stated in the previous section, the modelling is conducted until the mass and the velocity reach zero. In comparison, MTH has the highest vapour pressure at the prescribed temperature which is then followed by ETH, KE, CA, JA, and MA fuels.

Each fuel is given the same initial conditions for both atomization and spray penetration process. All fuels droplets have increased its diameter slightly before it declines as shown in Fig. 1. All biofuels have similar evaporating trends as Kerosene because they exhibit the same saturation vapour pressure correlation as in Kerosene and also other bulk physical properties such as bulk modulus, specific heat, and thermal conductivity [20]. Although MTH and ETH

fuels have higher vapour pressure, but the droplets have slower vaporization rate due to high vaporization latent heat which prevent an increase in temperature in the droplets. This is consistent with the work of [13]. When every droplet particles stopped, ETH fuel has the largest droplet particle reduction followed by MTH and KE fuels. All three biofuels have more than 50% diameter reduction before it stopped. Furthermore, JA fuel has the largest remaining droplet diameter, followed by MA, and CA biofuels. Average evaporation rate is taken by the gradient of each droplet fuel trend line. The average gradient showed that ETH has the highest value which corresponds to higher evaporation rate. These followed by MTH, CA, MA, JA and KE. As expected, that alternative fuels can contribute to less emission due to higher evaporation rate as compared to KE.

Transient variations of spray penetration process of various alternative fuels are plotted in Fig. 2. Spray penetration is an important parameter for combustor design, size and geometry since it will provide a significant effect on the engine performance and emission. Numerous soot will form as a result of the short penetration due to fuel coke [19]. All fuel exhibits the same trends as discussed in the literature where all fuels accelerated rapidly at the early stage and propagate at almost a constant speed. When the particle stops, MTH propagates the farthest distance followed by ETH and KE fuels. However, all biofuels have shorter penetration length. Yet, these cost penalties to the biofuels which exhibit more emissions in the existing combustors. Therefore, necessary engine design geometry need to be taken carefully to overcome soot formations.

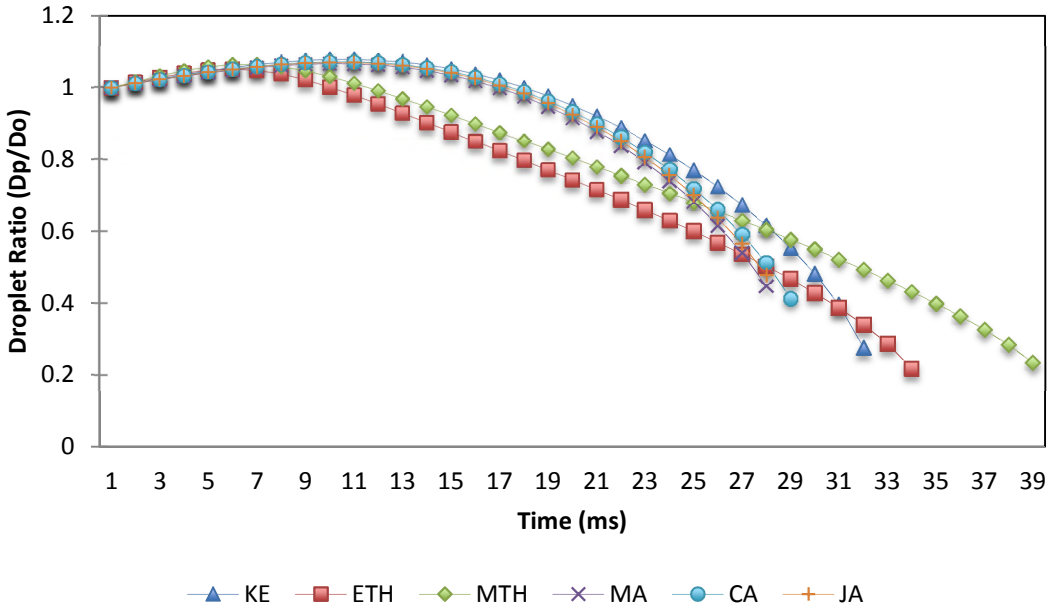

Fig. 1 Transient condition of evaporation process for each fuel

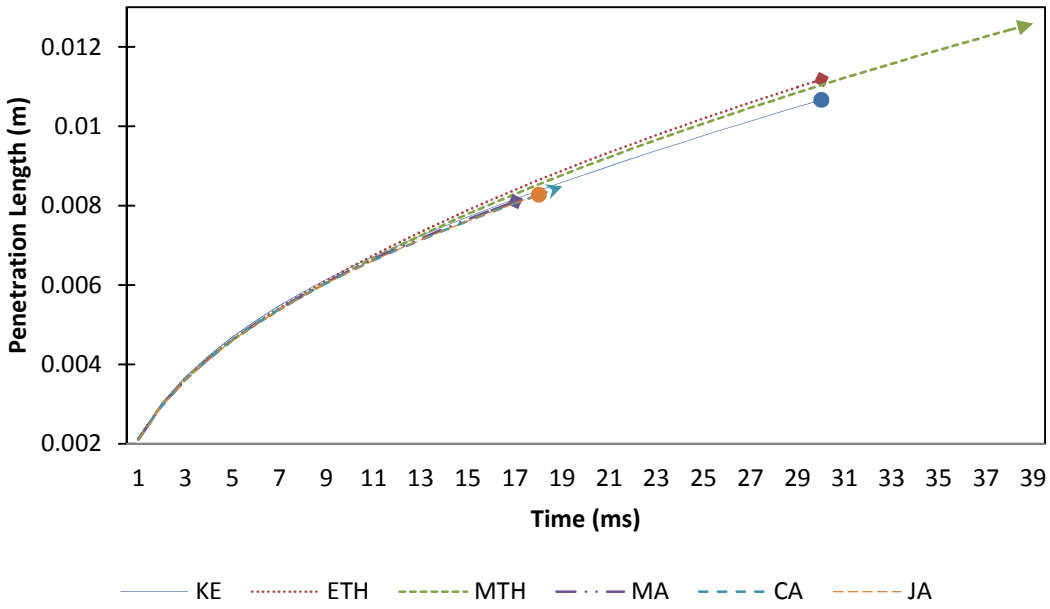

Fig. 2 Transient condition of penetration process for each fuel

The transient condition of temperature and density for each fuel are presented in Fig. 3 and Fig. 4. It was observed that there is an increase in temperature for all fuels but remained constant at a certain time. However, each fuel shows different constant temperatures where ETH has the lowest constant temperature while KE achieved the highest constant temperature. All biofuels

appeared to have an almost similar constant temperature. Notably, the changes of droplet's temperatures are determined in equation (16). Factors such as the latent heat, viscosity, evaporation rate (changes of mass) and molecular weight of the fuels influence the change in temperature. In contrast, density is reduced to a certain value until it reaches a certain point before it remains constant. The changes in fuel density are reflected by the change of temperature and particle velocity.

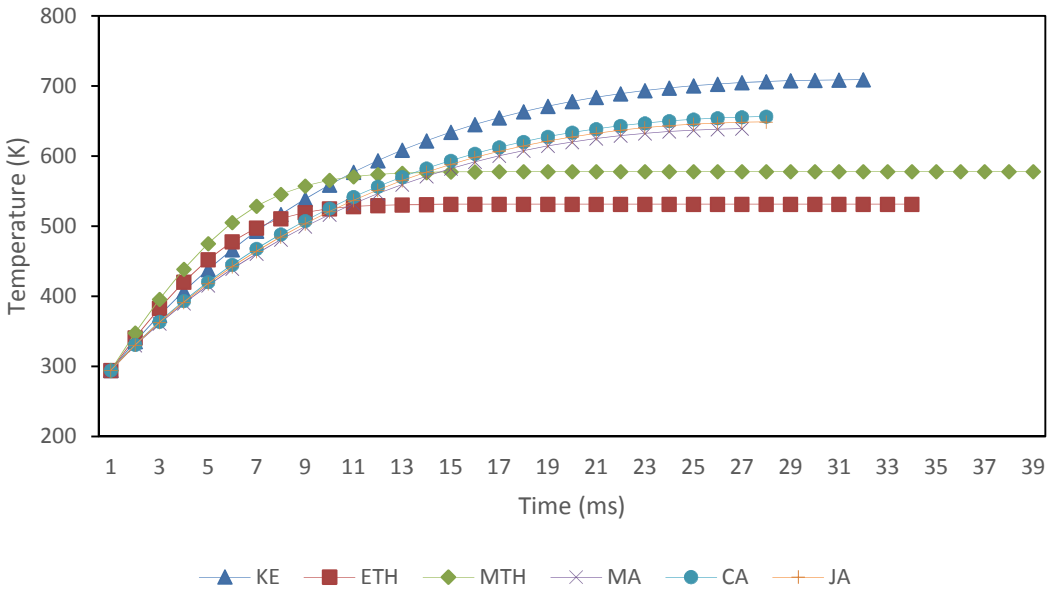

Fig. 3 Transient condition of temperature variation for each fuel

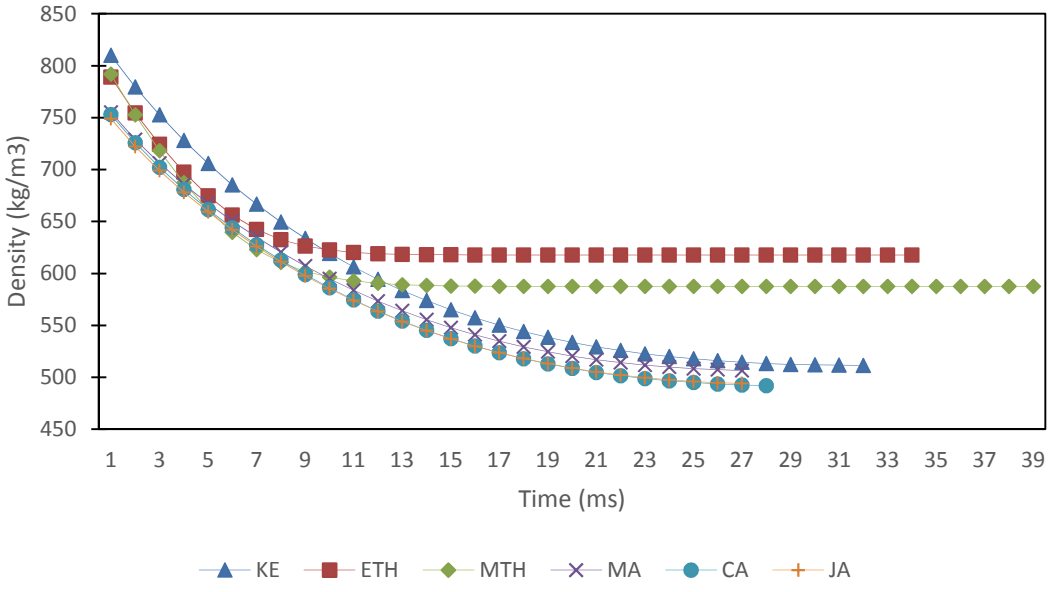

Fig. 4 Transient condition of density variation for each fuel

4.2 The influence of initial conditions on atomization and penetration

This section discusses the effects of various initial conditions such as different initial temperature and velocity of the droplet particle which have significant effects on the atomization and penetration process. Only KE fuel is closely examined and discussed. In the later paragraphs, different alternative fuels are compared and analyzed, having higher initial temperature and velocity. KE fuel droplet is given a prescribed time until the droplet particle stops. High initial temperature is preferable as it accelerates evaporation rate and exhibits greater changes to the droplet diameter resulting in a much smaller droplet diameter in a shorter time. These higher energy-contained droplet particles could enhance the mass transfer to the surrounding. On the other hand, high initial temperature also reduced the droplet particle's velocity much faster as illustrated in Fig. 5. However, it resulted in a low penetration length as shown in Fig. 6 and stopped much earlier. Penetration length of a high energy-contained droplet is reduced as the droplet is completely vaporized.

Similarly, high initial velocity has resulted in a much higher diameter gradient which indicates a higher evaporation rate. This is due to the higher mass transfer rate from the droplet surface to the surrounding. Although it has a much higher evaporation rate, but high-velocity droplet penetrates much longer before it stops. Their primary influences appear in the inertial forces. However, droplet particles at high velocity also appear to have a lesser amount of time to stop. The drag forces substantially play a dominant role as the velocity increases. Variations of different initial velocity are illustrated in Fig. 7 and Fig. 8 for evaporation and penetration processes. Therefore, it concluded that higher droplet velocities have shown faster evaporation rate and longer penetration length.

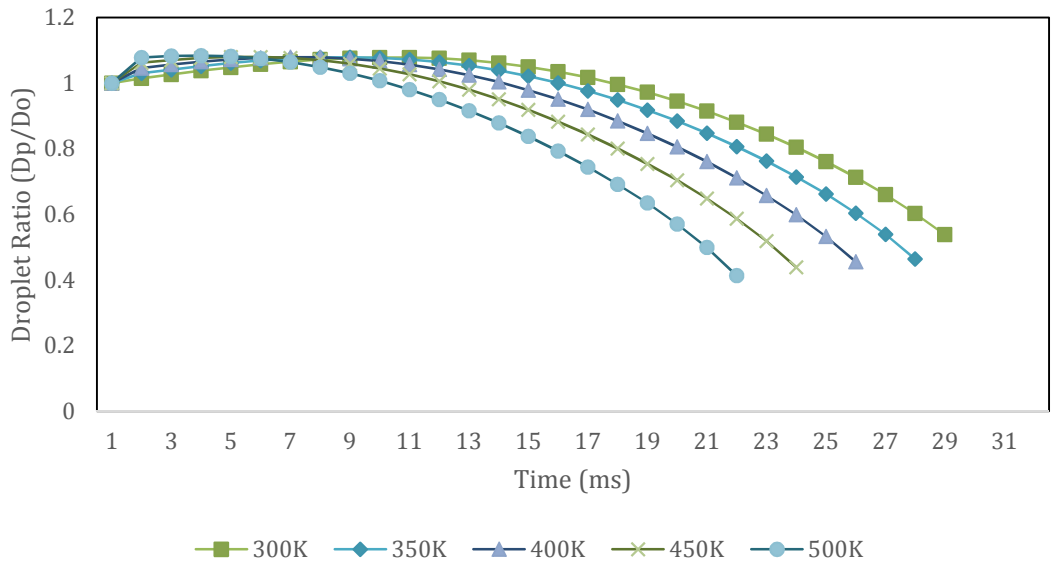

Fig. 5 Transient condition of evaporation process for KE under the influence of different temperatures

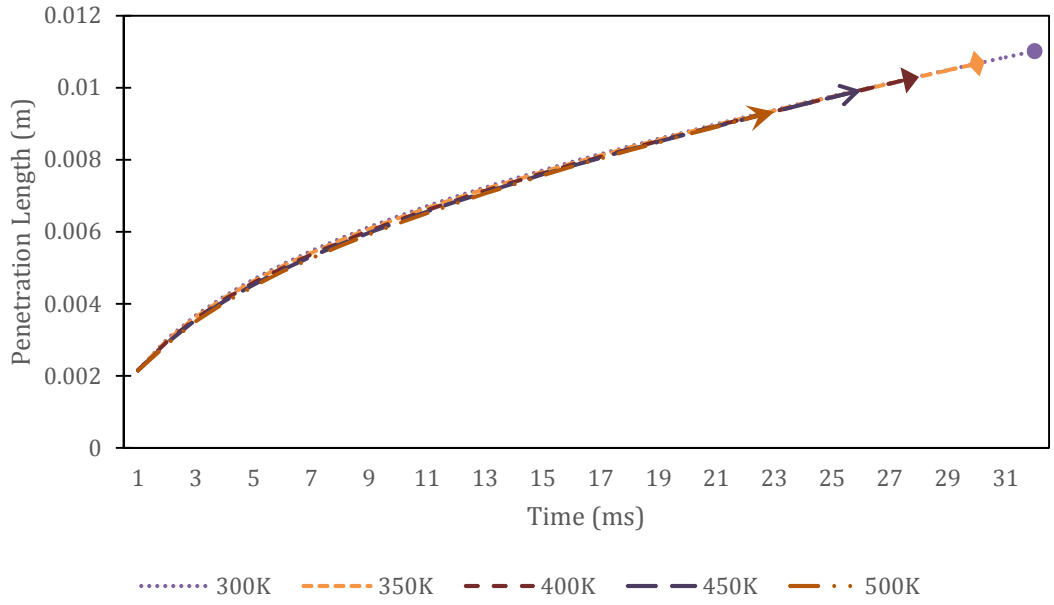

Fig. 6 Transient condition of penetration process for KE under the influence of different temperatures

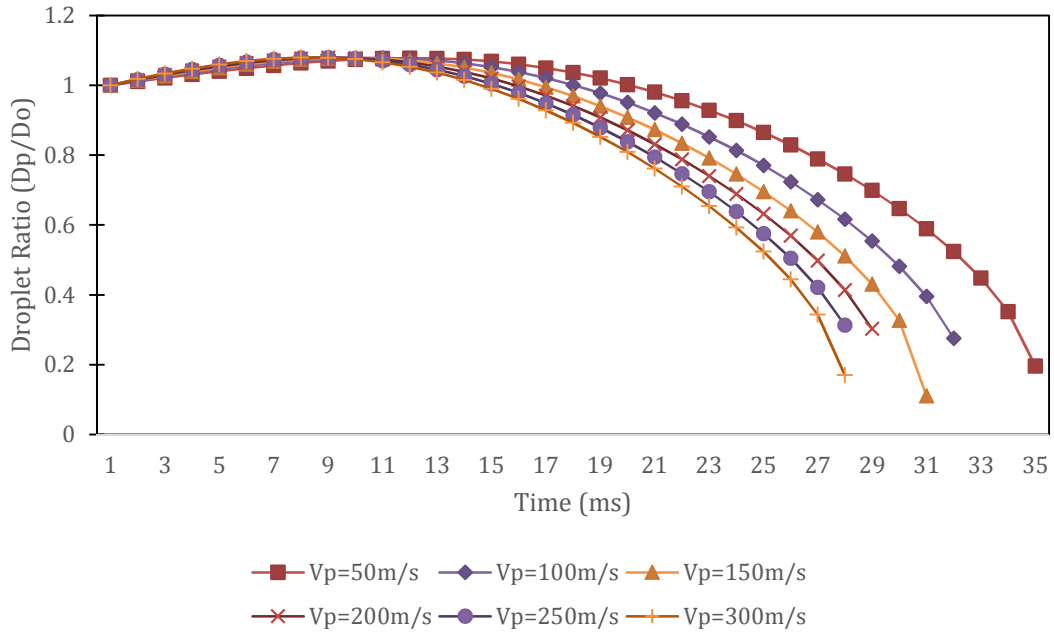

Fig. 7 Transient condition of evaporation process for KE under the influence of different initial velocity

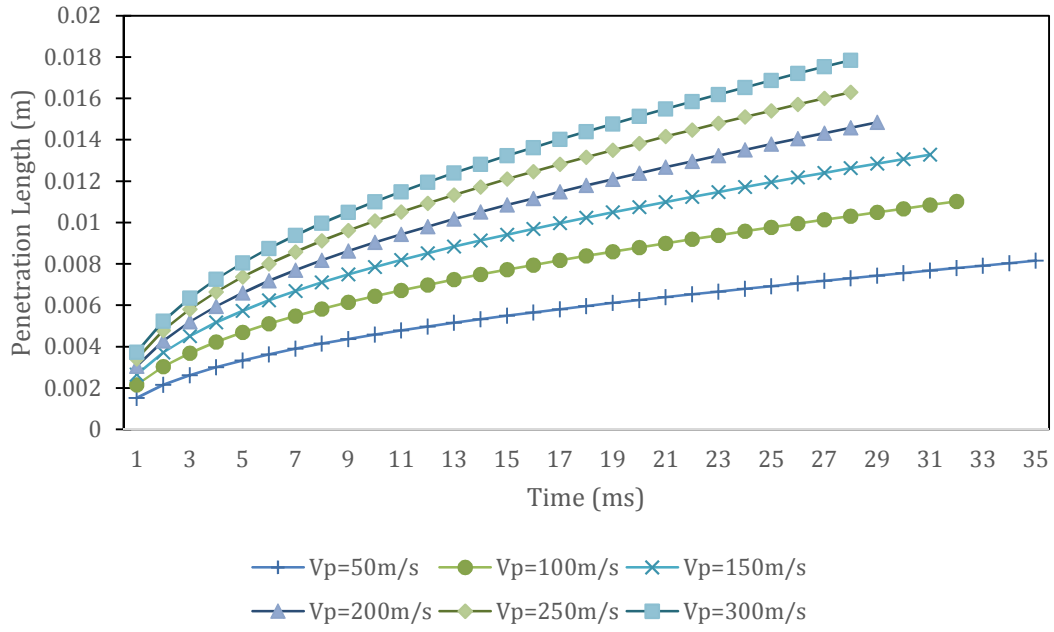

Fig. 8 Transient condition of penetration process for KE under the influence of different initial velocity

Evaporation and penetration process of different alternative fuels are compared and illustrated in Fig. 9 to Fig. 12. Firstly, we shall see the effects of high initial temperature towards both processes. Each fuel is heated to 500K

and modelled in a transient condition. The behaviour of these fuels is almost similar to the one obtained in Fig. 1 and Fig. 2. However, it should be highlighted again that higher initial temperature reduced the time for the droplet to stop and enhanced the evaporation rate as the gradient is much larger. However, only MTH fuel is almost completely vaporized when the droplet particle stopped. Meanwhile, other fuels showed that the diameter of the droplets is reduced more than 50%. Among all the biofuels, JA fuel has much more diameter reduction. The difference is that all fuels appear to have greater diameter reduction in a much shorter time at high initial temperature.

When the particles are accelerated to a higher velocity, evaporation rate is not increased. These can be shown in the slope of the plotted graphs in Fig. 11 as compared to Fig. 9. Higher initial velocity could reduce the time for the droplet to stop due to the increase of drag. The change of droplet diameter is much greater for KE, ETH and MTH fuels in a shorter time. On the other hand, other fuels, MA, CA and JA showed almost the same changes in droplet diameter as in lower initial velocity but, at a much shorter time. However, it permits the droplet to penetrate much longer as inertial forces become a dominant factor.

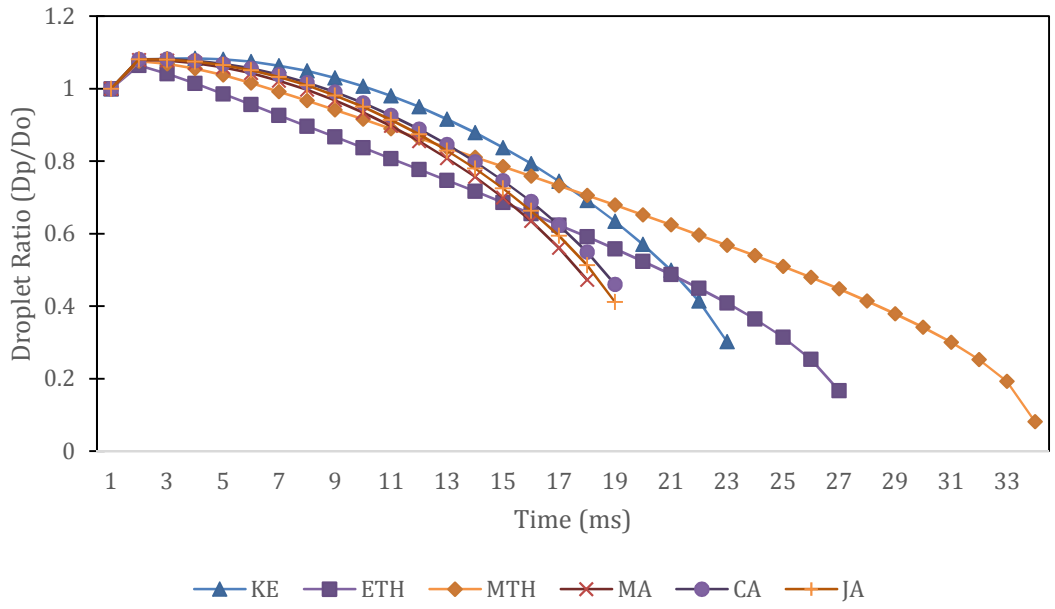

Fig. 9 Comparison of evaporation process for alternative fuels at higher initial temperature (Tp=500K)

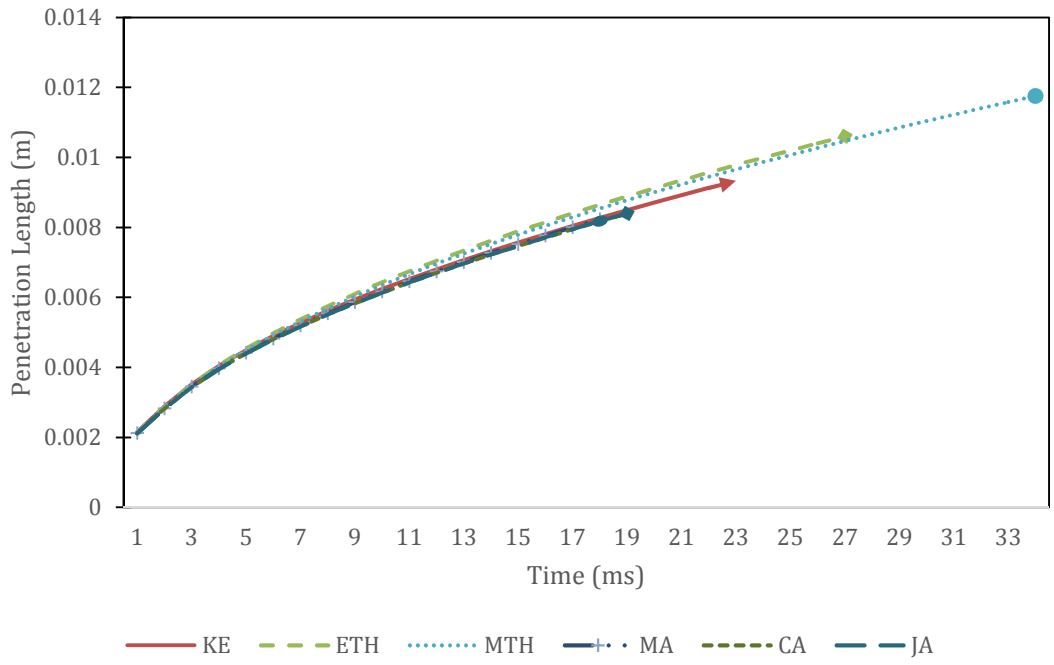

Fig. 10 Comparison of penetration process for alternative fuels at higher initial temperature (Tp=500K)

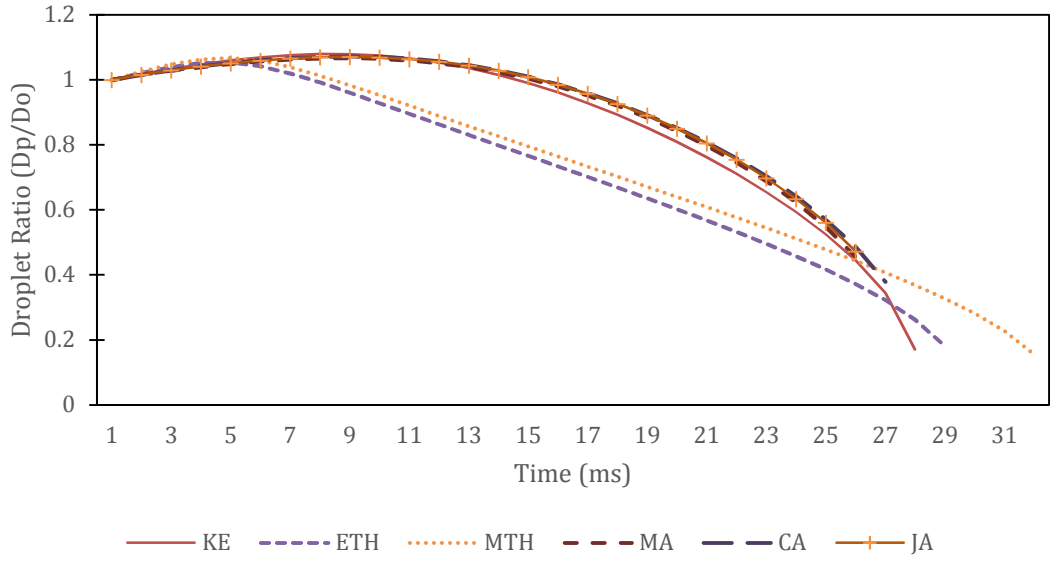

Fig. 11 Comparison of evaporation process for alternative fuels at higher initial velocity (Vp=300m/s)

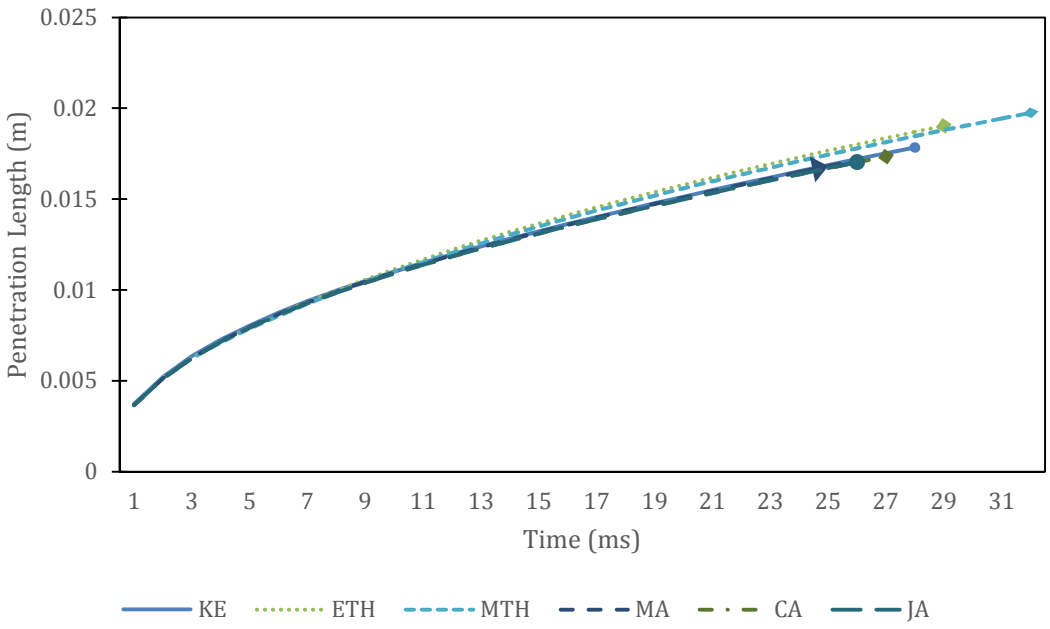

Fig. 12 Comparison of penetration process for alternative fuels at higher initial velocity (Vp=300m/s)

5. CONCLUSION

The focus of this work was on the modelling of evaporation and spray penetration for alternative fuels. Detailed comparisons have been made to visualize the transient behaviour of these fuels. The main conclusions of the work are:

1. An approximate expression for evaporation modelling is derived from FLUENT and to predict the length of penetration of the droplet by using Mazlan [22] and Sazhin et al. [12] correlation in transient conditions.
2. The vapour pressure tendencies have significant effects on the transient shape of the evaporation process. ETH fuel has the highest evaporation rate, followed by MTH, CA, MA, JA, and KE at room temperature.
3. At a given time, MTH droplet particle propagates the farthest distance and is followed by ETH and KE fuels. However, all biofuels have shorter penetration length in the given time. These give penalty costs to biofuels emissions formation.
4. The characteristics behaviour of temperature and density properties of droplet fuel have been estimated in a transient condition. Both

parameters showed a reverse pattern and achieve constant values at a particular time. Each fuel has different constant value since each fuel has different thermochemical properties.

5. The influence of initial conditions such as different temperatures and velocity are discussed. High initial temperature and velocity are preferable as they accelerate evaporation rate and exhibit greater changes to the droplet diameter resulting in a much smaller droplet diameter in a shorter time. Moreover, these initial conditions exhibit a much faster reduction on droplet particle's velocity. However, high initial temperature resulted in low penetration length, while high initial velocity permits the farthest penetration.

ACKNOWLEDGEMENTS

The first author acknowledges the sponsorship by International Islamic University Malaysia for funding his Ph.D. studies.

REFERENCES

[1] Amin S. Review on biofuel oil and gas production processes from microalgae. Energy Conversion and Management. Elsevier Ltd; July 2009; 50(7): 1834–1840. Available at: DOI:10.1016/j.enconman.2009.03.001

[2] Ashraful AM., Masjuki HH., Kalam MA., Fattah IMR., Imtenan S., Shahir SA., et al. Production and comparison of fuel properties , engine performance , and emission characteristics of biodiesel from various non-edible vegetable oils : A review. Energy Conversion and Management. Elsevier Ltd; 2014; 80: 202–228. Available at: DOI:10.1016/j.enconman.2014.01.037

[3] Atabani AE., Silitonga AS., Badruddin IA., Mahlia TMI., Masjuki HH., Mekhilef S. A comprehensive review on biodiesel as an alternative energy resource and its characteristics. Renewable and Sustainable Energy Reviews. Elsevier Ltd; May 2012; 16(4): 2070–2093. Available at:

DOI:10.1016/j.rser.2012.01.003

[4] Maity JP., Bundschuh J., Chen C-Y., Bhattacharya P. Microalgae for third generation biofuel production, mitigation of greenhouse gas emissions and wastewater treatment: Present and future perspectives – A mini review. Energy. Elsevier Ltd; April 2014; Available at: DOI:10.1016/j.energy.2014.04.003

[5] Giakoumis EG., Rakopoulos CD., Dimaratos AM., Rakopoulos DC. Exhaust emissions of diesel engines operating under transient conditions with biodiesel fuel blends. Progress in Energy and Combustion Science. Elsevier Ltd; 2012; 38(5): 691–715. Available at: DOI:10.1016/j.pecs.2012.05.002

[6] Padmanabhan MR A., Stanley SA. Microalgae as an Oil Producer for Biofuel Applications. Research Journal of Recent Sciences. 2012; 1(3): 57–62.

[7] Hoekman SK., Broch A., Robbins C., Ceniceros E., Natarajan M. Review of biodiesel composition , properties , and specifications. Renewable and Sustainable Energy Reviews. Elsevier Ltd; 2012; 16(1): 143–169. Available at: DOI:10.1016/j.rser.2011.07.143

[8] Giakoumis EG. A statistical investigation of biodiesel physical and chemical properties , and their correlation with the degree of unsaturation. Renewable Energy. Elsevier Ltd; 2013; 50: 858–878. Available at: DOI:10.1016/j.renene.2012.07.040

[9] Ejim CE., Fleck B a., Amirfazli a. Analytical study for atomization of biodiesels and their blends in a typical injector: Surface tension and viscosity effects. Fuel. 2007; 86: 1534–1544. Available at: DOI:10.1016/j.fuel.2006.11.006

[10] Chen P-C., Wang W-C., Roberts WL., Fang T. Spray and atomization of diesel fuel and its alternatives from a single-hole injector using a common rail fuel injection system. Fuel. Elsevier Ltd; 2013; 103(x): 850–861. Available at: DOI:10.1016/j.fuel.2012.08.013

[11] Ghosh S., Hunt JCR. Induced Air Velocity within Droplet Driven Sprays. Proceedings: Mathematical and Physical Sciences, Vol 444, No. 1920.

The Royal Society; 1994. pp. 105–127.

[12] Sazhin SS., Feng G., Heikal MR. A model for fuel spray penetration. Fuel. December 2001; 80(15): 2171–2180. Available at: DOI:10.1016/S0016-2361(01)00098-9

[13] Gu X., Basu S., Kumar R. Dispersion and vaporization of biofuels and conventional fuels in a crossflow pre-mixer. International Journal of Heat and Mass Transfer. Elsevier Ltd; 2012; 55(1-3): 336–346. Available at: DOI:10.1016/j.ijheatmasstransfer.2011.09.025

[14] Yule AJ., Filipovic I. On the Break-Up Times and Lengths of Diesel Sprays. International Journal of Heat and Fluid Flow. 1992; 13: 197–206. Available at: DOI:10.1016/0142-727X(92)90028-8

[15] Ryu J., Kim H., Lee K. A study on the spray structure and evaporation characteristic of common rail type high pressure injector in homogeneous charge compression ignition engine. Fuel. 2005; 84: 2341–2350. Available at: DOI:10.1016/j.fuel.2005.03.032

[16] Kostas J., Honnery D., Soria J. Time resolved measurements of the initial stages of fuel spray penetration. Fuel. Elsevier Ltd; 2009; 88(11): 2225–2237. Available at: DOI:10.1016/j.fuel.2009.05.013

[17] Lee CS., Park SW. An experimental and numerical study on fuel atomization characteristics of high-pressure diesel injection sprays. Fuel. 2002; 81: 2417–2423. Available at: DOI:10.1016/S0016-2361(02)00158-8

[18] Roisman IV., Araneo L., Tropea C. Effect of ambient pressure on penetration of a diesel spray. International Journal of Multiphase Flow. 2007; 33: 904–920. Available at: DOI:10.1016/j.ijmultiphaseflow.2007.01.004

[19] Mazlan NM., Savill M., Kipouros T. Computational Evaluation and Exploration of Combustion Performance for Liquid Jet Fuels Derived from Biomass. 3rd CEAS Air & Space Conference. Venice; 2011.

[20] Lefebvre HA., Ballal DR. Gas Turbine: Alternative Fuels and Emissions. 3rd edn. Florida: CRC Press; 2010.

[21] Morsi S., Alexander A. An investigation of particle trajectories in two-phase flow systems. J. Fluid Mech. 1972; 55: 193–208. Available at: DOI:10.1017/S0022112072001806

[22] Mazlan NM. Assessing/Optimising Bio-Fuel Combustion Technologies for Reducing Civil Aircraft Emissions. PhD Thesis Cranfield University; 2012.

[23] Ghassemi H., Baek SW., Khan QS. Experimental Study on Evaporation Ofkerosene Droplets At Elevated Pressuresand Temperatures. Combust.Sci.and Tech. 2006; 178(October): 1669–1684. Available at: DOI:10.1080/00102200600582392